Sustainable Energy Technologies and Assessments 66 (2024) 103804

Contents lists available at ScienceDirect

Sustainable Energy Technologies and Assessments

journal homepage: www.elsevier.com/locate/seta

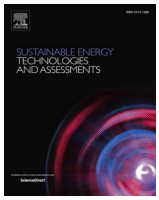

Original article

A modular IGBT power stack – based and open hardware framework for small wind turbines assessment

Jesus Clavijo-Camacho, Gabriel Gomez-Ruiz, Francisco J. Ruiz-Rodriguez, Reyes Sanchez-Herrera *

Department of Electrical Engineering, University of Huelva, Huelva, Spain

ARTICLE INFO

Keywords:
Small Wind Turbines
Experimental platform
Permanent Magnet Synchronous Generator (PMSG)
Machine Characterization
IGBT Power Stack
DC-DC Boost Converter

ABSTRACT

Wind energy technologies have emerged as the predominant renewable energy source within the framework of present-day electric power systems. Their design process, aligned with foundational theories, ought to be precision-engineered and systematized to fully maximize the potential of this energy source. This study presents a platform as solution designed and built to characterize and assess Small Wind Turbines (SWT), based on free software and open hardware. Additionally, the developed methodology step-by-step guide is disclosed. The characterization is based on the use of Permanent-Magnet Synchronous Generator (PMSG) as machine widely adopted in Wind Energy Conversion System (WECS) less than 100 kW. The core theoretical background is detailed to confirm the accuracy of the parameters procedures acquisitions. Poles number, machine design constant, armature reactance, synchronous reactance, and power-dynamic characteristic related to WECS are determined. This laboratory set-up is composed of variable industrial fan, rectifier, boost converter and a bidirectional Direct-Current (DC) source as a battery emulator. All components have been assembled within the laboratory environment using commercially available elements. Low implementation cost and versatile methods determine the real input in practice of this platform. To validate the effectiveness for any SWT, a real one is tested, and every parameter proposed is calculated.

Introduction

Given the present climate apprehension, multiple power generation systems are undergoing accelerated changes towards a decarbonized mix by 2050 [1] thus fulfilling what was agreed in the EU 2030 Agenda for Sustainable Development, specifically in "increase substantially the share of renewable energy in the global energy mix" [2]. This study research contributes directly to the initiatives and actions of this EU purpose by making a specific renewable energy system handier.

From final energy demand per sector in EU27 + UK in 2022, the demand in residential and industry sectors represented the 27 per cent and 25 per cent, respectively [3], that could be supplied by self-consumption introducing solar and SWT generation [4]. The efforts from EU governments are giving way to this distributed generation situation by promoting the small-scale installation [5].

In Spain, the energy mix generation is great compared to other EU countries given that the 42.2 per cent of the total energy generated in 2022 was from renewable sources [6] versus the 39.4 per cent as EU mean [7]. Focus on the wind energy, the 22.13 per cent generation in Spain was from this technology in contrast to the 15.9 per cent as mean in EU. In accordance to the data depicted, Spain as a member of the European Union, shows serious commitment and significant progress towards the aforementioned transition, in accordance with the guidelines and policies established at the European level [8] to address the issue.

The progression in this ecological transition involves the construction of new renewable generation [9] but prioritizing the design, analysis, and experimentation of the different technologies to be installed. The optimal exploitation of energies, specifically wind energy, constitutes the framework of the research presented in this paper, that will be based on the theory of electric machines, and on the use of power electronic applied to PMSG as the machine widespread used in WECS [10-12].

* Corresponding author.
E-mail address: reyes.sanchez@die.uhu.es (R. Sanchez-Herrera).

https://doi.org/10.1016/j.seta.2024.103804
Received 19 January 2024; Received in revised form 1 April 2024; Accepted 6 May 2024
Available online 11 May 2024

Literature overview

Upon conducting a literature review prior to the research, only one scientific and rigorously conducted article has been identified that exhibits a subtle alignment with the present research. In this context, the author in Verde et al. [13] emphasizes the importance of addressing the power losses to find real power curves of WECS but without providing the environment necessary to carry out the experiment, making it unreplicable. Furthermore, that study does not address a tangible necessity, and as a result, there is no practical implementation.

The existing literature lacks similar works to the one presented in this paper. This contribution fills a significant gap in the current scientific knowledge on wind energy, particularly in the domain of PMSG and their behaviour under variable wind speed conditions linked with the WECS that contain it. The absence of comparable research underscores the novelty and importance of the findings and insights put forth in this paper, thus enhancing the comprehension of synchronous machines and their operational characteristics applications.

The work addressed encompasses two key components parametrization: PMSG and WECS, so the literature overview must be divided into these fundamental subparts due to it has never been combined with the same purpose followed in this work.

On the one hand, there is a theoretical part on which the short-circuit and no-load studies of generators are based, and the characteristics that can be obtained from these tests. Synchronous generator and its analogues such as asynchronous generators, are subject of continuous research and evolution [14].The analysis of the armature reaction field is one of the most critical issues since it determines the efficiency and quality wave [15], the torque characteristic [16], vibration, and the acoustic noise [17], crucial in wind energy generation. The pole number correlates the machine speed and its momentum of inertia [18], so in variable wind speed it is decisive for considering the proper generation regime. Also, variation in the pole-pair impacts the achievement of different gear ratios [19] in multiple gear systems. For PMSG, the machine constat K stablishes the Back Electromotive Force (back-EMF) constant determining the generator efficiency and transient stability in faults [20], also, this K influences the torque produced in the generator and therefore the current flowing through its windings. In the process of designing generators for their incorporation into wind energy systems, it is essential to substantiate their design and construction establishing relationships among all factors that influence it.

On the other hand, the WECS themselves that inherently encompass the characteristics embedded within the PMSG behaviour. The outstanding field that concerns this study in WECS is the ability to: maximize the power extraction from the wind if it is required, and the adaptation to variable conditions. When delving into that field, two important characteristics are considered: the power performance curve C_p and the dynamic characteristic diagram. Although both represent similar concept, the power performance curve is specifically defined in terms of the tip-speed ratio [21] and it represents the relation between aerodynamics and wind energy. This characteristic can be obtained by using historical and recorded data [22,23] or by direct experimentation with the machine [24]. While a methodology exists for conducting studies of this nature focusing on WECS characteristics [25], its analysis of the generator and the interplay with its properties remains incomplete. Subsequently, advanced algorithms for the curve modelling and estimating has been developed [26,27]. In the methodology proposed in this paper, to simply relate the mechanical speed of the wind turbine to the final electric power it can produce, it is acquired the second characteristic named, the dynamic characteristic diagram for different wind speed [28,29].

The necessity of relating all of these parameters to wind speeds and operating regimes lies in the fundamental understanding of how the turbine's performance is influenced by environmental factors. The influence of wind speed on armature reaction and synchronous reactance, as well as the variation in rotational speed, is essential for comprehending the turbine's response to different wind speeds. This knowledge is crucial for the effective design, operation, and integration of wind turbines into power systems, ultimately contributing to the optimization of wind energy performance and reliability.

New contributions, applications, and paper organization

This research contributes in terms of novelty, originality, and significance in the following:

- Development of a testing procedure, step by step, for WECS characteristics acquisition.
- Design and implementation of a boost converter from a half-bridge IGBT topology commercial module for wind energy technology purpose.
- Constitution of a general and easy-to-construct WECS experimentation platform. Consisting of the variable industrial fan used to generate wind, rectifier, boost converter and its controller and the battery. The aim is to globalize it and make the study really reproduceable.
- Establishment of the theoretical performance of the PMSG in response to wind speed variations, validated through experimentation on a dedicated platform.

The proposed experimental platform allows characterizing wind turbines up to a power of 15 kW limited by the installed power converter, with the possibility of scaling it to higher power.

As solution of green energy transition, this platform contributes significantly to the design process of innovative wind-based electricity generation through the experimentation and with the consequent SWT characterization [30]. It would be possible to control the wind turbine at any of its operating points and to adapt any part of WECS rotor, stator, blades, bushing…etc. in a systematic manner. This means that any tests raised in WECS optimization can be conducted under control.

Furthermore, given the rigorous theoretical groundwork disclosed here, this platform can help university labs for the students gaining hands-on experience and apply theoretical knowledge in a real-world setting WECS [10]. Nowadays in teaching, the most used are simulation using PC software [31] or emulations by Alternating Current (AC) sources or those created by a semi-physical simulation testing bench [32,33]. All these types of WECS recreation will never be able to surpass the usable real system proposed here. Furthermore, prior to create a wind turbine simulator or emulator, it is necessary to base and validate it with real system models [34] and this platform can be also a solution in validation labours.

The paper is organized as follows. Theoretical foundations of PMSG and the relation to WECS in Section 2. The experimental set up for creating the platform and the procedures to acquire the parameters in Section 3. Experimental results in a case of use are presented and discussed in Section 4, and some conclusions are depicted in Section 5.

Theoretical foundations

Before addressing the characterization of a wind turbine, it is essential to expose the theoretical principles on which it is based. In this section, the equations, and relevant peculiarities of PMSG and WECS that are required for a comprehensive understanding of this experimental platform is presented in detail.

The wind generator is moved by the blades integrated into the rotor axis that will collect part of the power carried by the wind, P_w eq. (A.1) Appendix A. Consequently, the relationship between the power carried by the wind and the electrical output power P_e is outlined in eq. (A.2) Appendix A, where the C_P (power coefficient) will only depend on λ (tip speed ratio) as in SWT the pitch angle is uncontrollable. In the platform presented in this paper, the generator performance η_g considered in eq.

(A.2) Appendix A, also includes the friction when the shaft rotates, as in [35]. In [36] the author details the calculation of each loss for WECS.

For the platform created in the research presented in this paper, the characterization will be given by the relationship between the electrical power and the mechanical rotation speed of the machine, since the power coefficient mentioned above is intrinsically contemplated, this is called the dynamic characteristic of the machine.

Furthermore, by obtaining that characteristic curve it is possible to determine the optimum tip-speed ratio λ_{opt} for each wind speed, eq. (A.3) Appendix A. The optimum tip-speed ratio is the case when the power generated becomes maximum, or what is the same, Cp is maximum [37].

This approach makes feasible the determination of the maximum power that WECS is capable of produce for each wind speed.

As explained in *1. Introduction*, most small horizontal axis wind turbines are composed of a direct-drive PMSG. This type of generators does not have field excitation, therefore the electromotive force E_A is only proportional to the rotation speed ω_m during the entire operation of the machine for any connected load [38].

$$E_A = K \bullet \omega_m \tag{1}$$

The value of the voltage produced by the generator under load V_ϕ will be equal to the electromotive force generated with the existing speed E_A minus the voltage drop ΔV_{stator} produced by the resistance of the winding R_A and by the synchronous reactance [38].

$$\vec{V}_\phi = \vec{E}_A - \Delta\vec{V}_{stator} = \vec{E}_A - \vec{I}_A\,(R_A + jX_S) \tag{2}$$

Fig. 1 shows the equivalent circuit of PMSG per-phase. The synchronous reactance X_S is the sum of the self-inductance of the stator winding X_A and the armature reaction X.

$$X_S = X + X_A \tag{3}$$

The armature reaction is defined as the response or effect resulting from the interaction between the magnetic field generated by the magnets and the magnetic field induced by the machine stator.

Determining the reactance X_A is consistently possible by measuring the parameters below:

$$X_A = L_A \bullet 2 \bullet \pi \bullet f_{elect} \tag{4}$$

Being L_A the inductance of the stator winding and f_{elect} the electrical frequency of the generated voltage.

Due to the statement provided in eq. (1), through the platform presented in this study, the internal voltage of the machine can be calculated based on the voltage and the rotation speed measured with the generator in no-load operation. Since the electromotive force would be known for each rotation speed, it would be possible to estimate the voltage drops produced at any time with any connected load, eq. (2).

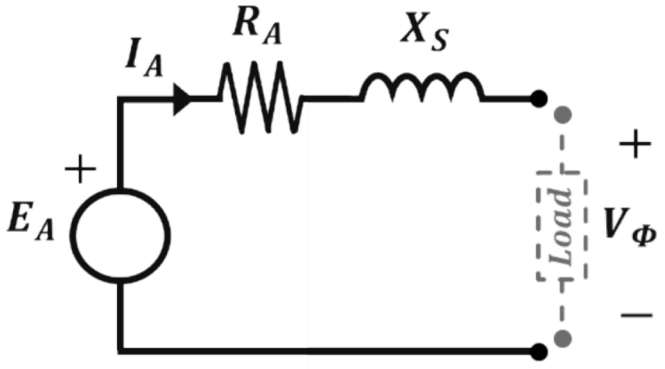

Fig. 1. Equivalent circuit of PMSG per-phase.

Furthermore, since the resistance of the stator winding R_A remains constant, the synchronous reactance X_S can be estimated. This makes possible to calculate the armature reaction X by using eq. (3) because X_A is defined for each value of f_{elect}, eq (4).

The design constant of the machine, k, and the magnetic flux, ϕ, created by magnets can be coined in a single term K. This parameter will have a proportional value and can be determined for each operating condition of the machine as another characteristic parameter in this testing platform. It will be observed that, being experimental, the measurement does not always remain at the same value, but it does have a trend.

As it is a generator composed of an inductor rotor where the permanent magnets are coupled, these will be organized in pairs. This important construction detail is called the number of pairs of rotor poles. The rotational speed ω_m at which the generator rotor rotates is related to the electrical frequency f_{elect} of the voltage generated and pole pairs P contained. This relationship is directly proportional, meaning that, if you increase the mechanical speed, the electrical frequency will also increase [39]:

$$P = \frac{f \bullet 60}{\omega_m} \tag{5}$$

Where P is the generator pairs of poles. To determine it, it is only needed to measure the electrical frequency f_{elect} of the generated voltage and the speed at which the rotor of the machine is rotating ω_m in that moment. The procedure of this calculation is shown in the next section.

Experimental set up and procedures

This section will be divided into two parts, the first one will detail the equipment necessary to start up the platform and the second part will explain the data acquisition procedure. This last subsection is in turn divided into the different parameters and characteristic curves of the generator that can be obtained.

Experimental set-up

In order to characterize any wind turbine, it is necessary to have a variable industrial fan controlled by a frequency converter that allows to generate and modify the resulting wind speed that will move the wind turbine, see Fig. 2.

The three-phase current is rectified by rectifier diodes, just before

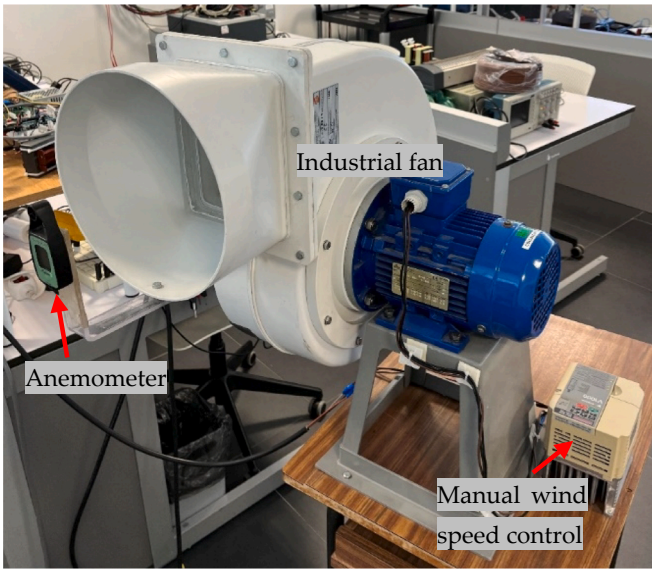

Fig. 2. Variable industrial fan used to generate wind.

this, it is necessary to place two wattmeters in Aron's connection [40] in order to measure the electrical power generated. Once the current is rectified, it flows through sensors installed in a Printed Circuit Board (PCB) designed ad hoc. Employing this PCB, it is possible to measure the power after the conversion to DC and monitor the WECS generation via PC. This data acquisition compromises the employment of a current transducer to measure the voltage (LEM LV 25-P) [41] and a non–invasive current sensor (LEM LA 55-P) [42], both signals are input into the Arduino MEGA controller [43] to be monitored from the computer. In Fig. 3, every stage is presented and in Fig. 4b) is schematized.

Arduino allows the possibility to generate the PWM signal that govern the IGBT incorporated in the converter. To create and modify this PWM signal, a simple code on Arduino has been designed with the use of a PWM library [44]. The duty cycle pulse width will be varied manually in order to test the wind turbine. In Fig. 4b) can be observe the device controlled by this signal.

This platform is conducted thanks to the power converter that can vary the working point of the wind turbine. It is a converter that raises the voltage from a lower level to a higher level, decreasing the current. To construct it, a Modular IGBT Power Stack from GUASCH company with reference MTM-1/2B2IC0225F12HB is used that incorporate a half bridge topology and capacitor bank C, Fig. 4a). This type of IGBT module is a constructive solution that allows for high versatility in creating customized IGBT power equipment. It consists of two IGBT designated T1 and T2. In the platform object of this work, the first IGBT will remain open while the second will be driven by the PWM signal generated by the Arduino. In Fig. 4a) the manufacturer's electronic schematic is shown and in b) the configuration adapted to build-up the necessary boost converter. To complete the boost converter built from the IGBT power stack, a L coil is connected at the input. Every parameter is indicated in Fig. 3 and its values depicted in Table B.1 of Appendix B. The value of the coil has initially been calculated in an analytical way [45] and then it has been empirically adapted to the tested wind turbine.

This IGBT has a switch frequency of 10 kHz, that is, it can switch every 0.0001 s. The output of the system will be connected to a battery emulated by a bidirectional source from the company EA Elektro Automatik, specifically the PSB 9000 model. This electronic instrument reproduces a real 350 V Li-Ion battery behavior which enable it works as energy source or sink. This device can be controlled mostly automatically by the software EA Battery Simulator during test runs. This is another essential feature of the setup to make it reproducible and versatile.

In addition to the above, the platform needs measurement instruments such as:

- Wattmeters connected at the output of the wind turbine to measure the three-phase power generated.
- Multimeters for measuring voltage and current, verifying the correct operation.
- Frequencymeter that measures the electrical frequency of the voltage wave generated by the generator.
- A tachometer to measure the speed of rotation of the shaft. This may be photodetector or contact.
- Oscilloscope that displays both the PWM signal and any other characteristic parameter of the machine. In the case of this platform, in addition to the PWM, the current in the coil and the voltage in the IGBT T2 are shown.

Data acquisition procedures

Once the necessary platform equipment has been detailed, the procedure to characterize the small wind generator will be disclosed below for each parameter.

Rotor winding poles numbers

As PMSG, the electrical frequency and the rotation speed of the rotor are related to the number of pairs of poles, as seen in eq. (5). Therefore, to calculate this last parameter it will be necessary to obtain the mechanical speed of the rotor ω_m and the electrical frequency of the wave f_{elect}, measured with a tachometer and frequency meter, respectively.

In generator no-load operation, a minimum of 2 measurements of each parameter are made and in each measurement the incident wind

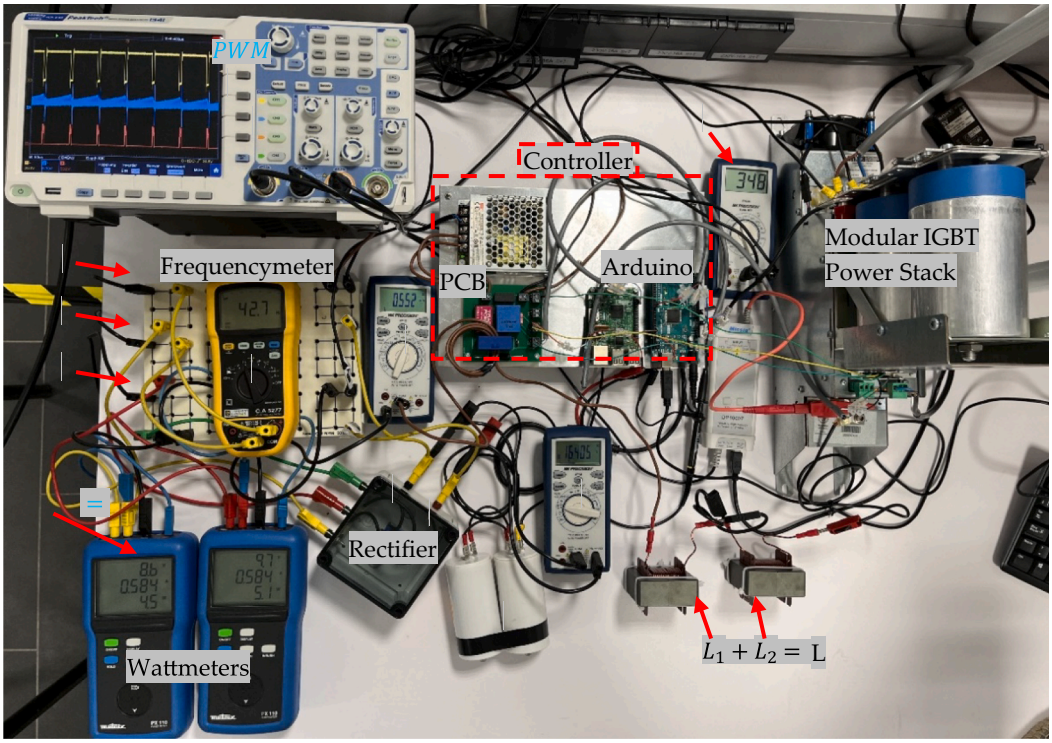

Fig. 3. Complete experimental set up of the platform presented.

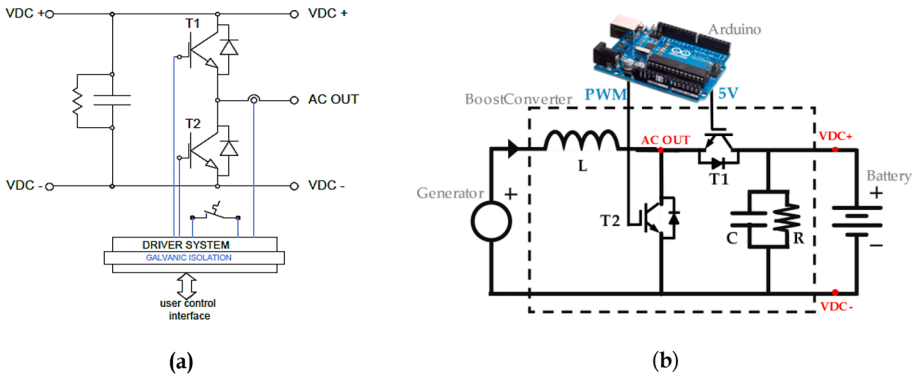

Fig. 4. Modular IGBT Power Stack scheme a) From manufacturer b) Boost Converter customized by adapting the half bridge topology equipment. Parameters values are disclosed in Appendix A.

speed will be change. Subsequently, applying the eq. (5) described in section 2. *Theoretical foundations* for each measurement, it is possible to obtain the number of pairs of poles, approaching the nearest integer.

PMSG design constant

The K constant of a PMSG takes on a fundamental role in the operation of the machine and, unless stated by the manufacturer, it remains unknown. To calculate it, as seen in eq. (1), it is enough to know the relationship between the electromotive force E_A generated by the machine and the rotational speed in the shaft. During generator in no-load condition, perform the following steps:

1. Set a wind speed with the industrial fan.
2. Let the stabilization of the wind turbine.
3. Measure the mechanical speed of the shaft, ω_m.
4. Measure the voltage on terminals between two phases, $V_{measure}$.

It is necessary to repeat the previous steps in a minimum range of wind speeds, the desirable would be from its speed cut-in to its speed cut-off. Depending on the configuration of the stator winding, the relationship between the measured voltage and the electromotive force may be as is indicated in Appendix B, eq (A.4) and (A.5).

When facing the values of E_A versus ω_m it will be possible to see how, being experimental, the values of this constant K oscillate, but always around the straight line that best fits the values taken, as will be shown in section 4. *Use Case*. In addition, the mean value for the parameter K is calculated by the zeroth moment, and it is also possible to obtain its standard deviation by calculating the square root of the second central moment. Based on these two data, mean and standard deviation, the construction constant of the PMSG is characterized.

PMSG armature reaction and synchronous reactance

The electromotive internal force E_A has already been obtained for each rotational speed in the previous subsection, now it would be possible to calculate by eq. (2) the voltage drop produced in the stator ΔV_{stator} just measuring V_ϕ for each mechanical speed of rotation ω_m with the rectifier, converter and battery already connected. It should be noted that, in the same way as before, when measuring the voltage between phases it is necessary to differentiate between the star or delta connection, but when current flows, the measured voltage $V_{measure}$ goes from having a relationship with E_A to V_ϕ. Fig. 1 schematizes what has been discussed.

Finally, as the resistance of the stator winding R_A can be measured and the stator current I_A can be quantified in each experiment with an ammeter, it is possible, therefore, to calculate the synchronous reactance X_S of the machine. This makes it possible to know the armature reaction X by means of eq. (3), due to X_A value is calculated for every f_{elect} eq. (4).

Establishing a wind speed and the no-load generator rotating at a settled speed, the conversion system is connected. Modifying the PWM will impose a load and cause the generator to rotate at different rotational speeds, the armature reaction X can be estimate for different incident wind speeds and different rotation speeds thanks to this modification of the PWM. The data collection process is visually represented in Fig. 5 via a flowchart.

An example of table to be fill in for the data collection procedure proposed will be shown in section 4. *Use Case*.

WECS dynamic characteristics curve

The extraction of the maximum power to be generated by this type of system inevitably involves performing a behaviour profile of the turbine for variable wind speed while varying rotational speed. This curve enables the establishment of an optimum tip-speed ratio λ_{opt} where the point of maximum conversion efficiency is reached. In SWT, the Maximum Power Point Tracker (MPPT) is set by controlling the electronic converter [46].

Carrying out the data collection described in Fig. 5, is it possible to obtain electric power P_{elect} versus rotational speed ω_m for each wind speed v_w tested. According to the flowchart provided, the rotational speed variation is made by the changeable PWM following the Duty Cycle, called *DutC* List, stablished.

The λ_{opt} is indicated in the dynamic characteristic curve obtained for the use case presented in this study.

Use case

According to the theoretical foundation, required set-up, and data acquisition procedure stablished in this study, the SWT platform has been developed. However, to corroborate these assumptions it is necessary to carry out real tests with a veritable SWT.

The wind turbine that is going to be characterize has horizontal axis, multi-bladed with six blades with a radius of 34 cm each, vane rudder and an uncontrollable pitch angle. The PMSG is coupled in the same shaft that make it rotates, which receives the torque generated by the turbine, therefore, it rotates at the same speed. Nevertheless, this speed differs from the voltage frequency generated that will depends on the poles number calculated below. The SWT tested is shown in Figure B.1 in Appendix B.

As indicated in the procedure to obtain the number of pairs of poles, the Table B.2 of empirical measurements for N° pairs of poles obtainment is shown in Appendix B.

It can be considered valid that the integer number of pairs of poles is four, indicated in the third column of Table B.2 in Appendix B. In WECS, the PMSG with a high number of pole pairs is certainly the most convenient for such applications because of its capability to operate at low speed without decreasing the efficiency, thus allowing to avoid gearbox [47]. In addition, the general rules of winding development for PMSG with the relevant restrictions are complied with [48].

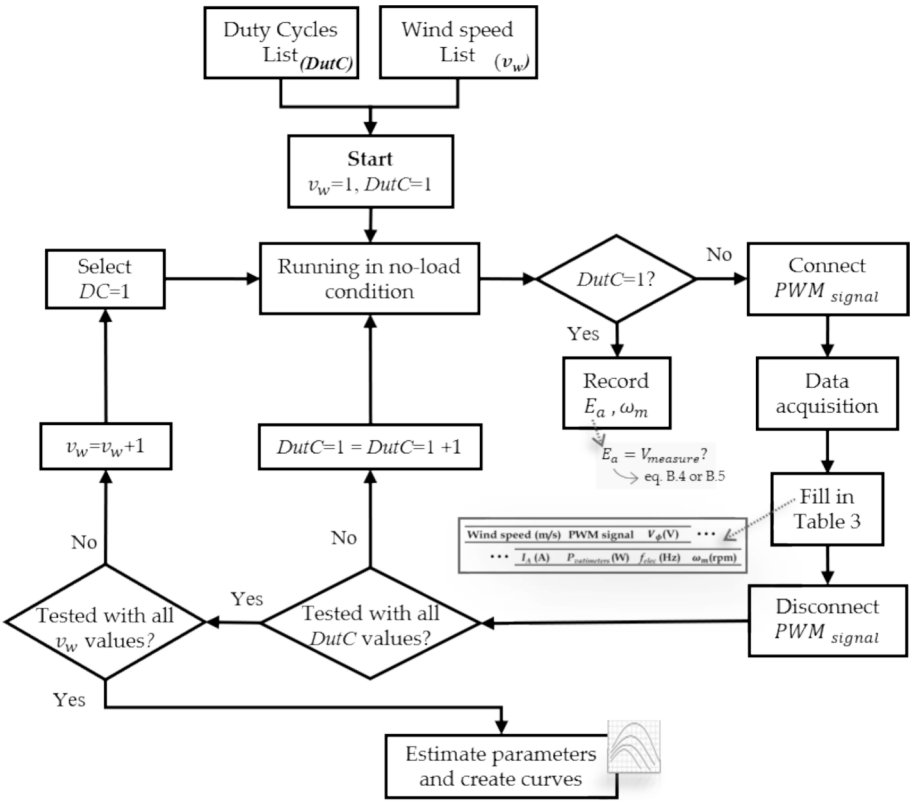

Fig. 5. Laboratory procedures for PMSG and WECS characterization.

The generator constant K is calculated for each sample using eq. (1) according to the procedure described in the corresponding section. The experimental values obtained as mean and standard deviation is depicted in Appendix B, Table B.3: For a total of thirteen samples, the scatter plot is shown in Fig. 6.

Since the standard deviation is of such a low order, the mean is consistent as the value of the constructive constant K of the machine. This value depends on the characteristics of the machine design, the geometry of the permanent magnets and the material used.

Fig. 7 shows the difference between the electromotive force given in non-load conditions and the voltage once the load is connected and for the different imposed wind speeds, as well as for the different rotation speeds of the rotor. It can be verified that the lower the wind speed, the lower the voltage drop in the stator due to a lower circulating current.

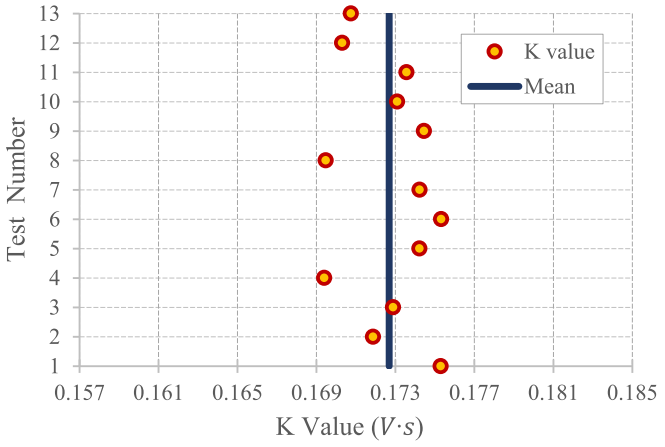

Fig. 6. Scatter Plot from different empirical measurements of machine constant K.

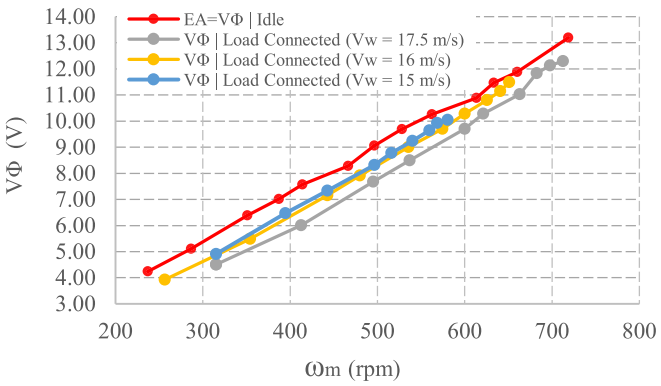

Fig. 7. Comparison of electromotive force in idle configuration with respect to the voltage once the load is connected.

Measuring the voltage drop, it is possible to calculate the synchronous reactance X_s. Next, due to that the reactance of the stator X_A is known for each rotor speed, the armature reaction X is calculated. Based on data presented in Table B.4. Appendix B (the experimental data collection for the SWT characterization from use case), in Fig. 8a) can be observe how the synchronous reactance X_s is the algebraic sum of the functions X_A observable in the Fig. 8b) and the armature reaction X Fig. 8c). As expected, the function X_A is linearly dependent on ω_m.

The resultant function X_s is the sum of a lineal X_A function and X function defined by the bivariate polynomial equation given in eq. (B.1) on Appendix B. Furthermore, the coefficient of this equation is appointed in Table B.5 of Appendix B. This X function demonstrates a non-lineal behaviour between armatures reaction and rotational speed. Concerning how armature reaction is influenced by the wind speed or available wind power, it is important to note that the value increases proportionally, but only slightly and maintain the same pattern for every

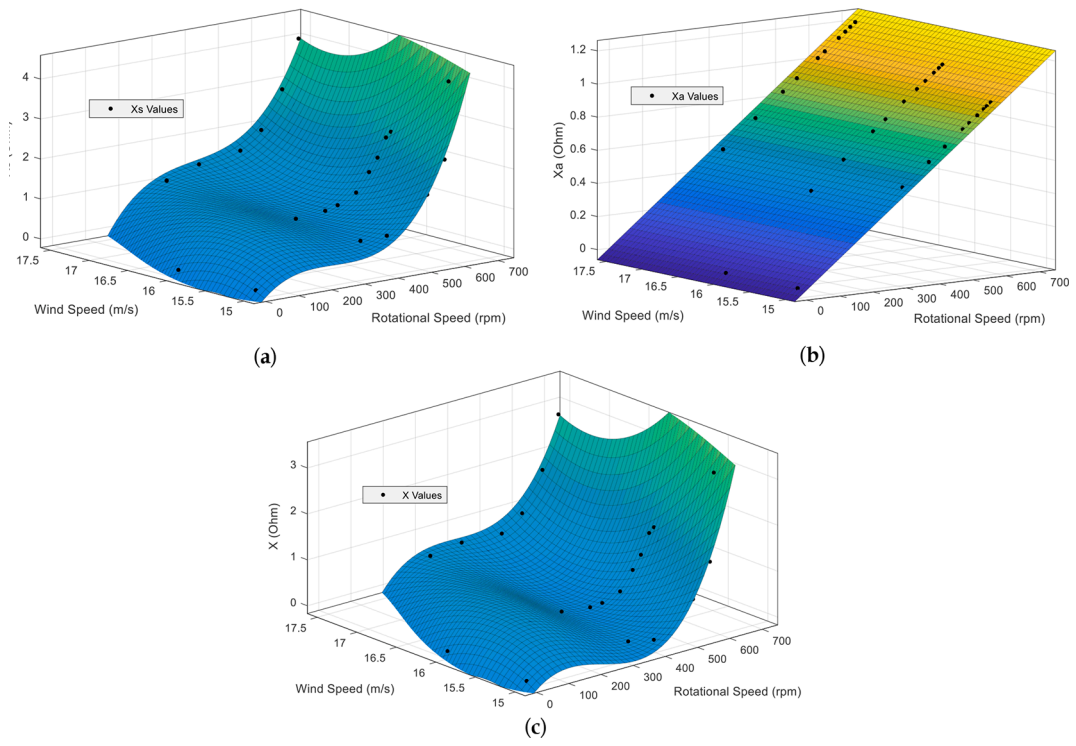

Fig. 8. Experimental results for different wind speeds and rotational speeds imposes by the converter. a) Synchronous Reactance, X_s b) Stator Inductance, X_A c) Armature Reaction, X.

wind speed as can be seen in Fig. 8c).

Finally, the characteristic curve of the WECS presented in this case study is obtained, in which the output power for different wind speeds is represented in Fig. 9. The MPPT is indicated with a black box, corresponding to the optimum tip-speed ratios λ_{opt}.

Conclusions

The comprehensive study has introduced an innovative and efficient methodology for experimentally evaluating small wind turbines (SWTs). The developed testing platform has demonstrated its efficacy as a valuable instrument for analyzing and understanding the performance

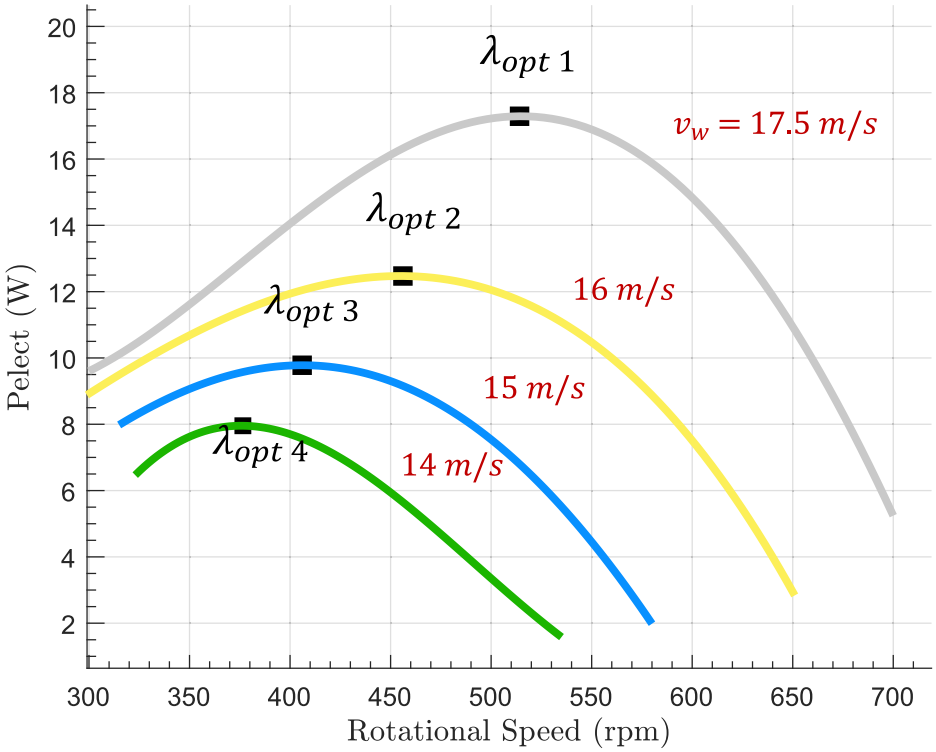

Fig. 9. $P_{elect} - \omega_m$ dynamic characteristic diagram for different wind speeds v_w.

of wind turbines under diverse wind conditions. The precise control of turbine speed, facilitated by a boost converter regulated from an Arduino microcontroller, has enabled the thorough characterization of the turbine's behavior. This research not only established a theoretical framework but also validated its practical applicability through experimental trials on a SWT.

In the context of the PMSG, the study has meticulously investigated the influence of varying wind speeds and rotational speeds on the armature reaction. This investigation has led to the determination of the resultant synchronous reactance through graphical representations and polynomial equations. Additionally, the study has encompassed the calculation of the number of poles and the design of the machine constant, establishing their correlation with the wind regime to achieve comprehensive machine characterization. The non-linear behavior of the generator through dynamic characteristic diagrams is exhibited, the graphics effectively illustrate the system's response to different rotational speeds under variable wind speed. This comprehensive analysis carries significant practical implications for the smooth integration of SWTs into electrical power systems.

The extension and scientific rigor of the study are underpinned by the practical application of the theoretical findings in a real-world setting, enabling the experimental validation of the testing platform and the acquisition of significant data for the characterization of SWTs. Furthermore, the emphasis on the reproducibility and adaptability of the platform highlights its relevance for ongoing research and development in real wind system environments.

CRediT authorship contribution statement

Jesus Clavijo-Camacho: Writing – original draft, Software, Methodology, Investigation, Conceptualization. **Gabriel Gomez-Ruiz:** Validation, Software, Data curation. **Francisco J. Ruiz-Rodriguez:** Writing – review & editing, Validation. **Reyes Sanchez-Herrera:** Investigation, Project administration, Supervision, Writing – review & editing.

Declaration of competing interest

The authors declare that they have no known competing financial interests or personal relationships that could have appeared to influence the work reported in this paper.

Data availability

Data will be made available on request.

Acknowledgments

Grant PID2020-117828RB-I00 "Integral control system to optimize the microgrids energy demand" funded by MICIU/AEI/10.13039/501100011033 and, by "Spanish Ministry of Science, Innovation and Universities". Additionally, Jesus Clavijo-Camacho is currently benefiting from an “INVESTIGO” research fellowship funded by the European Union - NextGenerationEU. Funding also for open access charge: Universidad de Huelva / CBUA.

Appendix A. – Additional equations for comprehensive research

The following equations correspond to the mathematical modelling of wind turbines.

The power carried by the wind collected by the blades:

$$P_w = \frac{1}{2}\rho_w A v_w^3 \tag{A.1}$$

Where A is the area swept by the turbine blades, ρ_w the air density and v_w the wind speed.

Relationship between the power carried by the wind and the electrical output power:

$$P_e = P_w \bullet C_P(\lambda) \bullet \eta_g \tag{A.2}$$

$C_P(\lambda)$ is the power coefficient characteristic of wind turbines that depends on the tip speed ratio λ and on the pitch angle β of the blades. Where η_g is the electric generator performance, which is induced by the copper and iron losses.

$$\lambda = \frac{R \bullet \omega_m}{v_w} \rightarrow \lambda_{opt} = \frac{R \bullet \omega_{mopt}}{v_w} \tag{A.3}$$

Where R is the blades radius and ω_m the mechanical rotor speed.

For the E_A measurement, if the connection is in star, then:

$$E_A = \frac{V_{measure}}{\sqrt{3}} \tag{A.4}$$

If the connection is in delta, then:

$$E_A = V_{measure} \tag{A.5}$$

Appendix B. – Related to the case of study

Table B.1. Parameter settings for rectification and voltage elevation conversion stages.

Parameter	Value
C_{rip}	99.25 mF
C	850 μF
L	6.8 mH
R	68 kΩ

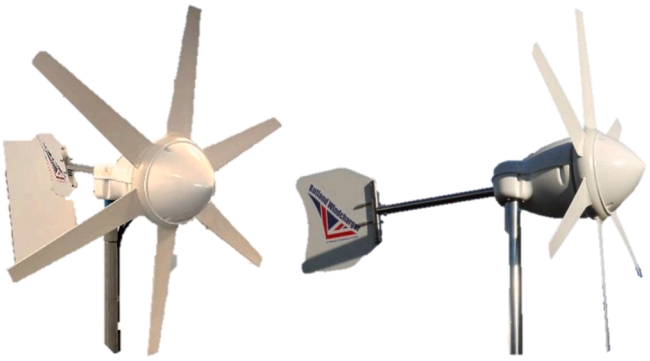

Figure B1. Small Wind Turbine to be characterized.

Table B.2. Empirical measurements for No. pairs of poles obtention.

Electrical frequency, f_{elect}	Mechanical speed, ω_m	No. pairs of poles (eq. 8)
45.5	686.3	3.97
35.8	545.5	3.93
27.5	406.8	4.05

Table B.3. Experimental Values obtained of machine constant *K*.

Mean ($V \bullet s$)	Standard Deviation ($V \bullet s$)
0.172681921	0.002033901

Table B.4. Experimental data collection for the SWT characterization from use case.

Wind speed (m/s)	Duty Cycle of PWM signal	$\boldsymbol{V_\phi}$(V)	I_A (A)	$P_{vatimeters}$ (W)	f_{elec} (Hz)	$\boldsymbol{\omega_m}$(rpm)
17.5	0.87	12.298	0.15	3.8	47.5	712.5
	0.88	12.124	0.2	5.4	46.5	697.5
	0.89	11.836	0.26	7.1	45.5	682.5
	0.9	11.027	0.33	9.8	44.2	663
	0.91	10.277	0.46	13.4	41.4	621
	0.92	9.699	0.54	15.1	40	600
	0.93	8.487	0.68	17	35.8	537
	0.94	7.679	0.82	17.1	33	495
	0.95	6.004	0.86	14.7	27.5	412.5
	0.96	4.503	0.79	10.5	21	315
	0.97	4.503	0.79	9.7	21	315
16	0.87	11.49	0.13	2.9	43.4	651
	0.88	11.14	0.17	4.1	42.7	640.5
	0.89	10.80	0.21	5.2	41.7	625.500
	0.9	10.28	0.27	7.2	40	600
	0.91	9.70	0.36	9.7	38.3	574.5
	0.92	9.01	0.43	10.8	35.7	535.5
	0.93	7.91	0.54	12.2	32	480
	0.94	7.16	0.63	12.7	29.5	442.5
	0.95	5.48	0.68	10.8	23.6	354
	0.96	3.93	0.62	7.1	17.1	256.5
15	0.87	10.05	0.106	2	38.7	580.5
	0.88	9.93	0.14	3	37.9	568.5
	0.89	9.64	0.169	3.7	37.3	559.5
	0.9	9.24	0.222	5	36	540
	0.91	8.78	0.29	6.6	34.4	516
	0.92	8.31	0.362	8	33.1	496.5
	0.93	7.33	0.47	9.4	29.5	442.5
	0.94	6.47	0.536	9.7	26.3	394.5
	0.95	4.91	0.58	8	21	315

The *X* resultant function for the SWT studied in the case studied is defined by:

$$X(\omega_m, v_w) = p_{00} + p_{10} \bullet \omega_m + p_{01} \bullet v_w + p_{20} \bullet {\omega_m}^2 + p_{11} \bullet \omega_m \bullet v_w + p_{02} \bullet {v_w}^2 + p_{30} \bullet {\omega_m}^3 + p_{21} \bullet {\omega_m}^2 \bullet v_w + p_{12} \bullet \omega_m \bullet {v_w}^2 \quad \text{(B.1)}$$

Table B.5. Coefficient of equation B.1.

Factor	Estimation
p00	−225.7
p10	0.5951
p01	29.21
p20	0.0001822
p11	−0.08146
p02	−0.9441
p30	6.222e-08
p21	−1.484e-05
p12	0.002815

References

[1] Hallste Pérez T, Rodríguez-Chueca J, Pérez Rodríguez J. Inclusion of key social indices for a comparative assessment of the sustainability of the life cycle of current and future electricity generation in Spain: a proposed methodology. Sci Total Environ 2023;899:165541. https://doi.org/10.1016/j.scitotenv.2023.165541.

[2] Weitz N, Carlsen H, Nilsson M, Skånberg K. Towards systemic and contextual priority setting for implementing the 2030 Agenda. Sustain Sci 2018;13(2):531–48. https://doi.org/10.1007/s11625-017-0470-0.

[3] 'Shedding light on energy in the EU: Production of electricity by source', Shedding light on energy in the EU: Production of electricity by source. Accessed: Mar. 25, 2024. [Online]. Available: https://ec.europa.eu/eurostat/cache/interactive-publications/energy/2024/05/index.html?simple=true.

[4] Bayod-Rújula ÁA, Haro-Larrodé ME, Martínez-Gracia A. Sizing criteria of hybrid photovoltaic–wind systems with battery storage and self-consumption considering interaction with the grid. Sol Energy 2013;98:582–91. https://doi.org/10.1016/j.solener.2013.10.023.

[5] Cerezo-Narváez A, Bastante-Ceca M-J, Piñero-Vilela J-M. Economic and environmental assessment on implementing solar renewable energy systems in Spanish residential homes. Energies 2021;14(14):14. https://doi.org/10.3390/en14144183.

[6] R. Eléctrica, 'REData - Generación', Red Eléctrica. Accessed: Oct. 24, 2023. [Online]. Available: https://www.ree.es/es/datos/generacion.

[7] 'How is EU electricity produced and sold?' Accessed: Oct. 24, 2023. [Online]. Available: https://www.consilium.europa.eu/en/infographics/how-is-eu-electricity-produced-and-sold/.

[8] 'Renewable energy directive'. Accessed: Oct. 24, 2023. [Online]. Available: https://energy.ec.europa.eu/topics/renewable-energy/renewable-energy-directive-targets-and-rules/renewable-energy-directive_en.

[9] Ramos C, García AS, Moreno B, Díaz G. Small-scale renewable power technologies are an alternative to reach a sustainable economic growth: Evidence from Spain. Energy 2019;167:13–25. https://doi.org/10.1016/j.energy.2018.10.118.

[10] Urtasun A, Sanchis P, San Martín I, López J, Marroyo L. Modeling of small wind turbines based on PMSG with diode bridge for sensorless maximum power tracking. Renewable Energy 2013;55:138–49. https://doi.org/10.1016/j.renene.2012.12.035.

[11] Freire NMA, Cardoso AJM. Fault-tolerant PMSG drive with reduced DC-link ratings for wind turbine applications. IEEE J Emerg Selected Top Power Electron 2014;2(1). https://doi.org/10.1109/JESTPE.2013.2295061.

[12] Hansen AD, Michalke G. Modelling and control of variable-speed multi-pole permanent magnet synchronous generator wind turbine. Wind Energy 2008;11(5):537–54. https://doi.org/10.1002/we.278.

[13] Verde A, Lastres O, Hernández G, Ibañez G, Verea L, Sebastian PJ. A new method for characterization of small capacity wind turbines with permanent magnet synchronous generator: An experimental study. Heliyon 2018;4(8):e00732. https://doi.org/10.1016/j.heliyon.2018.e00732.

[14] 'Future research directions for the wind turbine generator system', Renew Sustain Energy Rev 2015; 49: 481–9, doi: 10.1016/j.rser.2015.04.126.

[15] Kamiev K, Nerg J, Pyrhonen J, Zaboin V, Tapia J. Feasibility of an armature-reaction-compensated permanent-magnet synchronous generator in island operation. IEEE Trans Ind Electron 2014;61(9):5075–85. https://doi.org/10.1109/TIE.2013.2289871.

[16] Kim J-H, Tae-Song O, Ri Y-S, Kim S-H, Yun C-J. Reduction of quadrature armature reaction in salient-pole synchronous generator by rotor flux barrier. Electr Eng 2023. https://doi.org/10.1007/s00202-023-01955-8.

[17] Qiu Z, Chen Y, Liu X, Kang Y, Liu H. Analysis of the sideband current harmonics and vibro-acoustics in the PMSM with SVPWM. IET Power Electron 2020;13(5):1033–40. https://doi.org/10.1049/iet-pel.2019.0661.

[18] He L, Gu X, Han Y, Zhou Z, Tian X, Cheng G. Nonlinear dual action piezoelectric energy harvester for collecting wind energy from the environment. J Alloy Compd 2021;889:161711. https://doi.org/10.1016/j.jallcom.2021.161711.

[19] Li W, Chau KT, Lee CHT, Ching TW, Chen M, Jiang JZ. A new linear magnetic gear with adjustable gear ratios and its application for direct-drive wave energy extraction. Renew Energy 2017;105:199–208. https://doi.org/10.1016/j.renene.2016.12.026.

[20] Okedu KE, Al Tobi M, Al Araimi S. Comparative study of the effects of machine parameters on DFIG and PMSG variable speed wind turbines during grid fault. Front Energy Res 2021;9:681443. https://doi.org/10.3389/fenrg.2021.681443.

[21] Ganjefar S, Ghassemi AA, Ahmadi MM. Improving efficiency of two-type maximum power point tracking methods of tip-speed ratio and optimum torque in wind turbine system using a quantum neural network. Energy 2014;67:444–53. https://doi.org/10.1016/j.energy.2014.02.023.

[22] Long H, Wang L, Zhang Z, Song Z, Xu J. Data-driven wind turbine power generation performance monitoring. IEEE Trans Ind Electron 2015;62(10):6627–35. https://doi.org/10.1109/TIE.2015.2447508.

[23] Jing H, Zhao C. Adjustable piecewise regression strategy based wind turbine power forecasting for probabilistic condition monitoring. Sustain Energy Technol Assess 2022;52:102013. https://doi.org/10.1016/j.seta.2022.102013.

[24] Edwards JM, Angelo Danao L, Howell RJ. Novel experimental power curve determination and computational methods for the performance analysis of vertical axis wind turbines. J Solar Energy Eng 2012;134(3):031008. https://doi.org/10.1115/1.4006196.

[25] 'Performance characterisation of a commercial-scale wind turbine operating in an urban environment, using real data', Energy Sustain Dev 2017; 36: 44–54, doi: 10.1016/j.esd.2016.11.001.

[26] Lydia M, Selvakumar AI, Kumar SS, Kumar GEP. Advanced algorithms for wind turbine power curve modeling. IEEE Trans Sustain Energy 2013;4(3):827–35. https://doi.org/10.1109/TSTE.2013.2247641.

[27] Mok K, 'Identification of the power coefficient of wind turbines', in *IEEE Power Engineering Society General Meeting, 2005*, Jun. 2005, pp. 2078-2082 Vol. 2. doi: 10.1109/PES.2005.1489074.

[28] Kavousi A, Fathi SH, Milimonfared J, Soltani MN. Application of boost converter to increase the speed range of dual-stator winding induction generator in wind power systems. IEEE Trans Power Electron 2018;33(11):9599–610. https://doi.org/10.1109/TPEL.2018.2797095.

[29] Xie J, et al. Characteristics simulation method of megawatt three-blade horizontal axis wind turbine based on laboratory kilowatt low-power motor system. IEEE Trans Ind Appl 2022;58(1):645–55. https://doi.org/10.1109/TIA.2021.3123116.

[30] Rudrapal D, Acharya S. Characterization of a novel lift-drag-driven air-activated hybrid vertical axis wind turbine. Sustain Energy Technol Assess 2023;59:103415. https://doi.org/10.1016/j.seta.2023.103415.

[31] Fragoso S, Ruz ML, Garrido J, Vazquez F, Morilla F. Educational software tool for decoupling control in wind turbines applied to a lab-scale system. Comput Appl Eng Educ 2016;24(3):400–11. https://doi.org/10.1002/cae.21718.

[32] Elbouchikhi E, Feld G, Amirat Y, Benbouzid M, Gall FL. Design and experimental implementation of a wind energy conversion platform with education and research capabilities. Comput Electr Eng 2020;85:106661. https://doi.org/10.1016/j.compeleceng.2020.106661.

[33] Navarro L, Christian G, Quintero M, Pardo M. 'A Lab-oriented Testing Platform for Emulating a Wind Turbine in a DC Microgrid', in *2020 IEEE Texas Power and Energy Conference (TPEC)*, Feb. 2020, pp. 1–6. doi: 10.1109/TPEC48276.2020.9042546.

[34] Kusiak A, Zheng H, Song Z. On-line monitoring of power curves. Renew Energy 2009;34(6):1487–93. https://doi.org/10.1016/j.renene.2008.10.022.

[35] Chapman SJ. Electric machinery fundamentals. 5th edition. New York: McGraw-Hill; 2012.

[36] De Kooning JDM, Gevaert L, Van de Vyver J, Vandoorn TL, Vandevelde L. 'Online estimation of the power coefficient versus tip-speed ratio curve of wind turbines', in *IECON 2013 - 39th Annual Conference of the IEEE Industrial Electronics Society*, Nov. 2013, pp. 1792–1797. doi: 10.1109/IECON.2013.6699403.

[37] Dursun EH, Kulaksiz AA. MPPT control of PMSG based small-scale wind energy conversion system connected to DC-Bus. Int J Emerg Electr Power Syst 2020;21(2):2. https://doi.org/10.1515/ijeeps-2019-0188.

[38] Chan TF, Lai LL. An axial-flux permanent-magnet synchronous generator for a direct-coupled wind-turbine system. IEEE Trans Energy Conversion 2007;22(1):86–94. https://doi.org/10.1109/TEC.2006.889546.

[39] Laxminarayan SS, Singh M, Saifee AH, Mittal A. Design, modeling and simulation of variable speed axial flux permanent magnet wind generator. Sustainable Energy Technol Assess 2017;19:114–24. https://doi.org/10.1016/j.seta.2017.01.004.

[40] Ing. T. Sezi, 'Fast and accurate measurement of power system frequency', in *IEEE PES General Meeting*, Jul. 2010, pp. 1–7. doi: 10.1109/PES.2010.5589297.

[41] 'LV 25-P SENSOR DATASHEET'. Accessed: Nov. 22, 2023. [Online]. Available: https://www.lem.com/sites/default/files/products_datasheets/lv_25-p.pdf.
[42] 'LA 55-P SENSOR DATASHEET'. Accessed: Nov. 22, 2023. [Online]. Available: https://www.lem.com/sites/default/files/products_datasheets/la_55-p_e.pdf.
[43] 'Arduino - Home'. Accessed: Nov. 22, 2023. [Online]. Available: https://www.arduino.cc/.
[44] Mueller L, Mohammed M, Kimball JW. Using the Arduino Uno to Teach Digital Control of Power Electronics. in 2015 IEEE 16th Workshop on Control and Modeling for Power Electronics (COMPEL), in IEEE Workshop on Control and Modeling for Power Electronics. New York: IEEE; 2015. Accessed: Oct. 30, 2023. [Online]. Available:.
[45] Rahimi M. Modeling, control and stability analysis of grid connected PMSG based wind turbine assisted with diode rectifier and boost converter. Int J Electr Power Energy Syst 2017;93:84–96. https://doi.org/10.1016/j.ijepes.2017.05.019.
[46] Kesraoui M, Korichi N, Belkadi A. Maximum power point tracker of wind energy conversion system. Renew Energy 2011;36(10):2655–62. https://doi.org/10.1016/j.renene.2010.04.028.
[47] Mirecki A, Roboam X, Richardeau F. Architecture complexity and energy efficiency of small wind turbines. IEEE Trans Ind Electron 2007;54(1):660–70. https://doi.org/10.1109/TIE.2006.885456.
[48] Cistelecan MV, Popescu M, Popescu M. 'Study of the Number of Slots/Pole Combinations for Low Speed Permanent Magnet Synchronous Generators', in *2007 IEEE International Electric Machines & Drives Conference*, May 2007, pp. 1616–1620. doi: 10.1109/IEMDC.2007.383671.